NANO LETTERS

2007
Vol. 7, No. 10
3065−3070

Quantum Dot–Aptamer Conjugates for Synchronous Cancer Imaging, Therapy, and Sensing of Drug Delivery Based on Bi-Fluorescence Resonance Energy Transfer

Vaishali Bagalkot,[†,‡] Liangfang Zhang,[§] Etgar Levy-Nissenbaum,[†,§] Sangyong Jon,[*,‡] Philip W. Kantoff,[||] Robert Langer,[§] and Omid C. Farokhzad[*,†]

Laboratory of Nanomedicine and Biomaterials and Department of Anesthesiology, Brigham and Women's Hospital, Harvard Medical School, Boston, Massachusetts 02115, Research Center for Biomolecular Nanotechnology, Department of Life Science, Gwangju Institute of Science and Technology, Buk-gu, Gwangju 500-712, South Korea, Department of Chemical Engineering, Massachusetts Institute of Technology, Cambridge, Massachusetts 02139, and Lank Center for Genitourinary Oncology, Dana Farber Cancer Institute, Harvard Medical School, Boston, Massachusetts 02115

Received June 28, 2007; Revised Manuscript Received August 21, 2007

ABSTRACT

We report a novel quantum dot (QD)–aptamer(Apt)–doxorubicin (Dox) conjugate [QD–Apt(Dox)] as a targeted cancer imaging, therapy, and sensing system. By functionalizing the surface of fluorescent QD with the A10 RNA aptamer, which recognizes the extracellular domain of the prostate specific membrane antigen (PSMA), we developed a targeted QD imaging system (QD–Apt) that is capable of differential uptake and imaging of prostate cancer cells that express the PSMA protein. The intercalation of Dox, a widely used antineoplastic anthracycline drug with fluorescent properties, in the double-stranded stem of the A10 aptamer results in a targeted QD–Apt(Dox) conjugate with reversible self-quenching properties based on a Bi-FRET mechanism. A donor–acceptor model fluorescence resonance energy transfer (FRET) between QD and Dox and a donor–quencher model FRET between Dox and aptamer result when Dox intercalated within the A10 aptamer. This simple multifunctional nanoparticle system can deliver Dox to the targeted prostate cancer cells and sense the delivery of Dox by activating the fluorescence of QD, which concurrently images the cancer cells. We demonstrate the specificity and sensitivity of this nanoparticle conjugate as a cancer imaging, therapy and sensing system in vitro.

Semiconductor nanocrystals known as quantum dots (QDs) have been increasingly utilized as biological imaging and labeling probes because of their unique optical properties, including broad absorption with narrow photoluminescence spectra, high quantum yield, low photobleaching, and resistance to chemical degradation. In some cases, these unique properties have conferred advantages over traditional fluorophores such as organic dyes.[1−4] The surface modification of QDs with antibodies, aptamers, peptides, or small molecules that bind to antigens present on the target cells or tissues has resulted in the development of sensitive and specific targeted imaging and diagnostic modalities for in vitro and in vivo applications.[5−7] More recently, QDs have been engineered to carry distinct classes of therapeutic agents for simultaneous imaging and therapeutic applications.[8,9] While these combined imaging therapy nanoparticles represent an exciting advance in the field of nanomedicine, it would be ideal to engineer "smart" multifunctional nanoparticles that are capable of performing these tasks while sensing the delivery of drugs in a simple and easily detectable manner. One way to achieve this goal is to develop multifunctional nanoparticles capable of sensing the release of the therapeutic modality by a change in the fluorescence of the imaging modality. It would be important to maintain simplicity in design and engineering to ensure the possible

* Corresponding authors. E-mail: syjon@gist.ac.kr (S.J.); ofarokhzad@zeus.bwh.harvard.edu (O.C.F.).

[†] Laboratory of Nanomedicine and Biomaterials and Department of Anesthesiology, Brigham and Women's Hospital, Harvard Medical School.

[‡] Research Center for Biomolecular Nanotechnology, Department of Life Science, Gwangju Institute of Science and Technology.

[§] Department of Chemical Engineering, Massachusetts Institute of Technology.

[||] Lank Center for Genitourinary Oncology, Dana Farber Cancer Institute, Harvard Medical School.

10.1021/nl071546n CCC: $37.00
Published on Web 09/14/2007

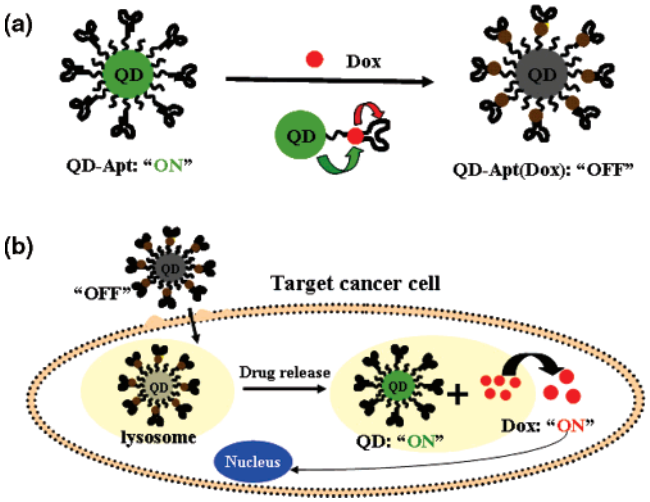

Figure 1. (a) Schematic illustration of QD−Apt(Dox) Bi-FRET system. In the first step, the CdSe/ZnS core−shell QD are surface functionalized with the A10 PSMA aptamer. The intercalation of Dox within the A10 PSMA aptamer on the surface of QDs results in the formation of the QD−Apt(Dox) and quenching of both QD and Dox fluorescence through a Bi-FRET mechanism: the fluorescence of the QD is quenched by Dox while simultaneously the fluorescence of Dox is quenched by intercalation within the A10 PSMA aptamer resulting in the "OFF" state. (b) Schematic illustration of specific uptake of QD−Apt(Dox) conjugates into target cancer cell through PSMA mediate endocytosis. The release of Dox from the QD−Apt(Dox) conjugates induces the recovery of fluorescence from both QD and Dox ("ON" state), thereby sensing the intracellular delivery of Dox and enabling the synchronous fluorescent localization and killing of cancer cells.

development and scale-up of these systems for research and medical applications.

Herein, we report a novel and simple proof of concept QD−aptamer (QD−Apt) conjugate that can image and deliver anticancer drugs to prostate cancer (PCa) cells and sense the delivery of drugs to the targeted tumor cells based on the mechanism of fluorescence resonance energy transfer (FRET).[10,11] As illustrated in Figure 1a, the conjugate is comprised of three components: (i) QDs, which function as fluorescent imaging vehicles,[1−4] (ii) RNA aptamers covalently attached to the surface of QD, which serve a dual function as targeting molecules and as drug carrying vehicles,[12] and (iii) doxorubicin (Dox), which is a widely used anthracycline drug with known fluorescent properties that intercalates within the double-stranded CG sequences of RNA and DNA as a therapeutic agent.[13] The assembly of this system results in the formation of a Bi-FRET complex: [14] a donor−acceptor model FRET between QD and Dox, where the fluorescence of QD is quenched as a result of Dox absorbance, and a donor−quencher model FRET between Dox and aptamer, where Dox is quenched by double-stranded RNA aptamer. Therefore, both QD and Dox of the conjugate are in the fluorescence "OFF" state when the QD−Apt is loaded with Dox [QD−Apt(Dox)]. After the particle is taken up by targeted cancer cells, Dox is gradually released from the conjugate, which induces the activation of QD and Dox fluorescence to the "ON" state. This simple multifunctional nanoparticle system can potentially deliver Dox to the targeted cells and sense the delivery of Dox by activating

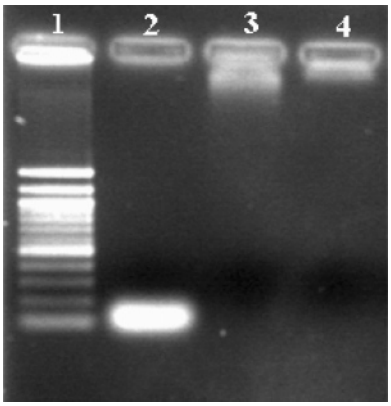

Figure 2. Gel electrophoresis results of QD−Apt conjugate after staining with ethidium bromide. Lanes 1, 2, 3, and 4 represent the 100 bp DNA ladder, A10 PSMA aptamer, QD−Apt conjugate, and QD alone, respectively.

the fluorescence of QD, which concurrently images the cancer cells (schematically represented in Figure 1b).

In this study, we used CdSe/ZnS core−shell QD490 as a model QD, and the A10 RNA aptamer, which binds to the prostate specific membrane antigen (PSMA) on the surface of PCa cells, as a model aptamer-targeting molecule.[15,16] The A10 PSMA aptamer is a 57 base pair nuclease-stabilized 2′-flouropyrimidine RNA molecule with a single 5′-CG-3′ sequence in its predicted double-stranded stem region that is the preferred binding site of Dox.[13,17] We have previously shown that incubation of Dox with the A10 PSMA aptamer results in the formation of a reversible physical conjugate, with a final Dox:Aptamer stoichiometry of 1:1.1, consistent with the intercalation of the Dox into a single CG sequence present in this aptamer.[17] It is well-known that the anthracycline class of drugs such as Dox has fluorescence properties.[18,19] The Dox molecules can be maximally excited by absorbing light with wavelength of 480 nm, resulting in the emission of light in the range of 520−640 nm. This enables Dox to act as the photon acceptor of CdSe/ZnS QD490, which emits light in the range of 470−530 nm. The CdSe/ZnS QD490 has a broad excitation wavelength, and in these studies, we used the wavelength 350 nm, which avoided the inadvertent excitation of Dox.

We first conjugated the amine-terminated A10 RNA aptamer to the surface of carboxyl-terminated QDs using 1-ethyl-3-(3-dimethylaminopropyl) carbodiimide (EDC) and *N*-hydroxysuccinimide (NHS) activation chemistry. Gel electrophoresis data in Figure 2 demonstrate the formation of the QD−Apt conjugates. Nonspecifically bound aptamers were efficiently washed off by using centrifugal filtration. After forming QD−aptamer conjugates, the extra carboxyl groups present on the QD surface were subsequently quenched by using ethanol amine to avoid nonspecific binding of positively charged Dox to the negative QD surface due to electrostatic attraction. We next incubated the QD−Apt conjugate with Dox to form QD−Apt(Dox) conjugates by intercalating Dox into the CG sequence present in PSMA aptamer.[15] We had previously shown that the intercalation of Dox within the A10 PSMA results in the quenching of Dox fluorescence through a donor−quencher model FRET

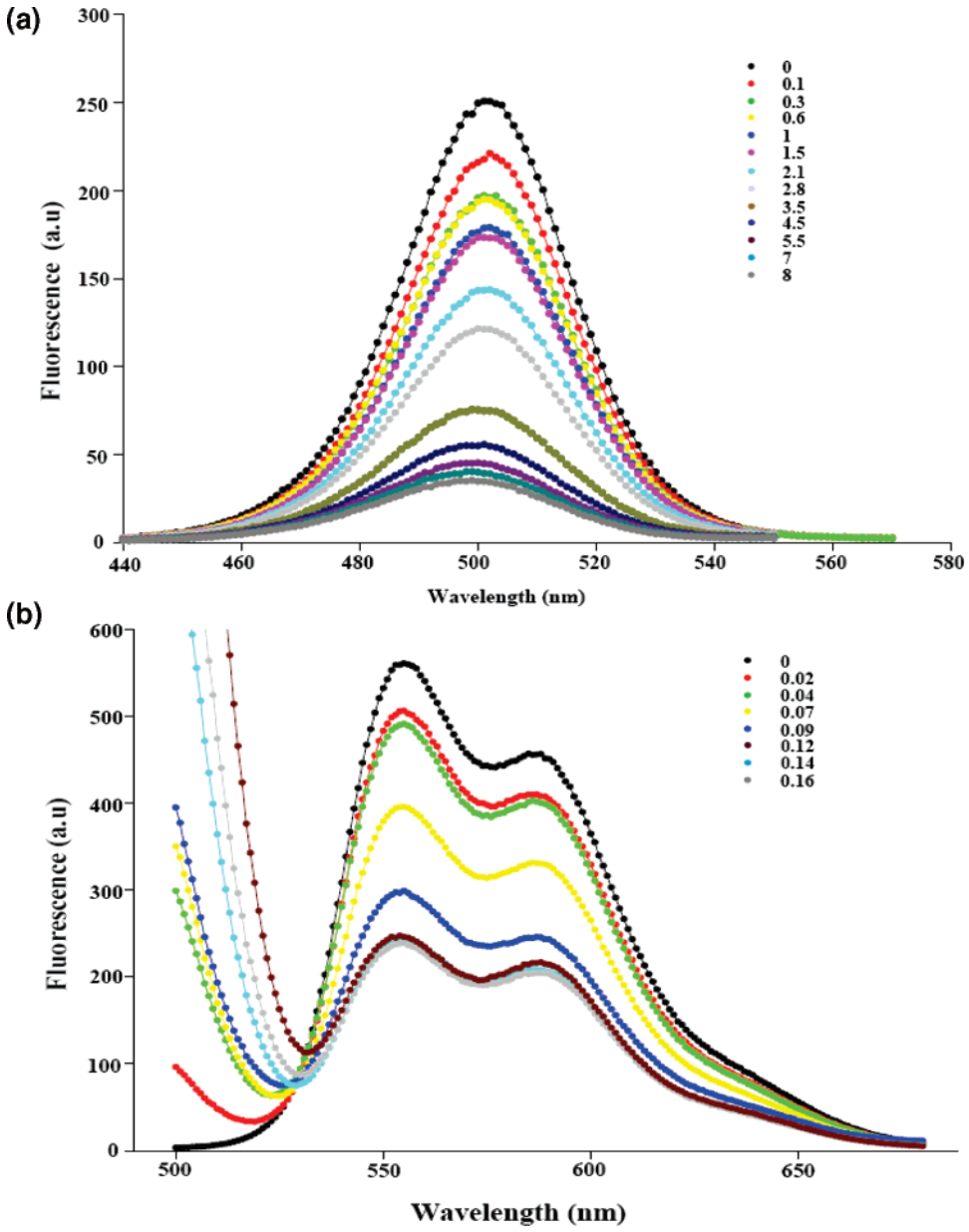

Figure 3. Fluorescence spectra. (a) QD−Apt conjugate (1 μM) with increasing molar ratio of Dox (from top to bottom: 0, 0.1, 0.3, 0.6, 1, 1.5, 2.1, 2.8, 3.5, 4.5, 5.5, 7, and 8) at an excitation of 350 nm. (b) Dox (10 μM) with increasing molar ratio of QD−Apt conjugate (from top to bottom: 0.02, 0.04, 0.07, 0.09, 0.12, 0.14, and 0.16) at an excitation of 480 nm.

between Dox and the A10 PSMA aptamer,[17] and herein we hypothesized that the presence of Dox intercalated on the surface of QD−Apt may result in quenching of QD through a donor−acceptor model FRET between the QD and Dox. To examine if such Bi-FRET system occurs, we used fluorescence spectroscopy to monitor the binding of Dox to QD−Apt conjugates. Sequential decreases in the fluorescence emission spectrum of QD were observed when a fixed concentration of QD−Apt conjugates (1 μM) was incubated with an increasing molar ratio of Dox (Figure 3a). This result suggests that Dox binding indeed causes energy transfer from QD to Dox, which diminishes the fluorescence of QD. Maximal quenching was observed at QD−Apt:Dox ratio of ~1:7, which suggests that on average seven Dox-loaded aptamer molecules are sufficient to maximally quench the QD fluorescence. It is possible that each QD−Apt conjugate carries additional aptamer and Dox molecules, which can augment the targeting and cytotoxic benefit of these conjugates without further quenching the QD fluorescence. Figure 3b demonstrates a similar sequential decrease of Dox emission when a fixed concentration of Dox (10 μM) was incubated with an increasing molar ratio of QD−aptamer conjugates. This observation confirms that the fluorescence emission of Dox can be quenched by intercalation within the A10 PSMA aptamer on the surface of QDs. Taken together, the data demonstrate the formation of the QD−Apt(Dox) conjugate resulting in a Bi-FRET system with potential application in PSMA expressing PCa cells.

We became interested in evaluating the specificity and sensitivity of the QD−Apt(Dox) conjugates as a combined imaging, therapy, and drug delivery sensing vehicles in vitro. As a first step, we examined whether QD−Apt conjugates

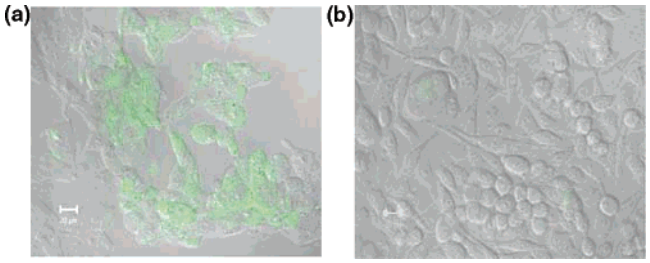

Figure 4. Binding of QD−Apt conjugates to (a) LNCaP (PSMA+), and (b) PC3 (PSMA−) prostate adenocarcinoma cells. QD is shown in green. The scale bar is 20 μm.

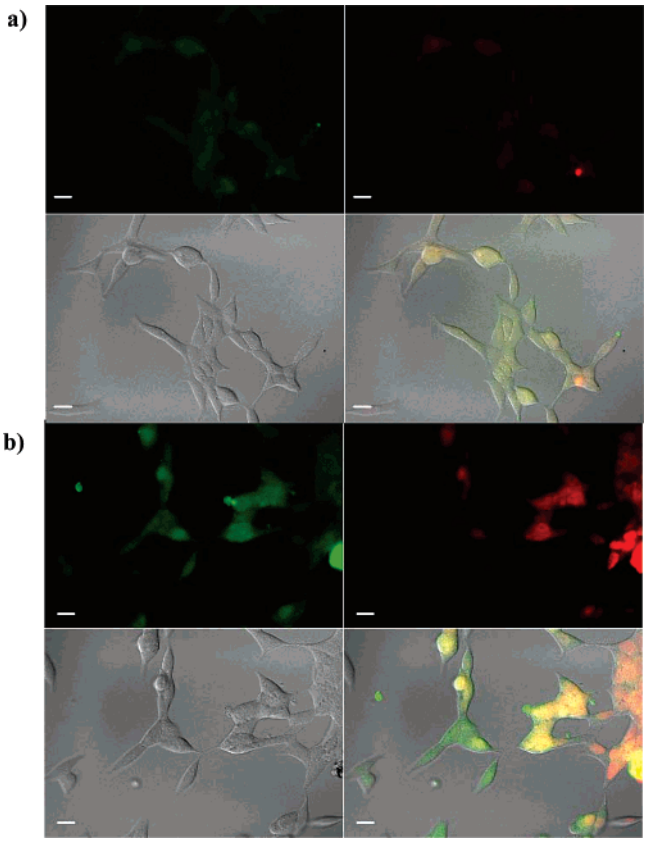

Figure 5. Confocal laser scanning microscopy images of PSMA expressing LNCaP cells after incubation with 100 nM QD−Apt-(Dox) conjugates for 0.5 h at 37 °C, washed two times with PBS buffer, and further incubated at 37 °C for (a) 0 h and (b) 1.5 h. Dox and QD are shown in red and green, respectively, and the lower right images of each panel represents the overlay of Dox and QD fluorescent. The scale bar is 20 μm.

can differentially bind to PSMA-expressing LNCaP but not the PSMA-negative PC3 prostate adenocarcinoma cell lines. Both cell lines were incubated with 100 nM QD−Apt conjugate for 0.5 h at 37 °C, followed by copious wash steps to remove unbound conjugates. Figure 4 demonstrates that QD−Apt conjugates were effectively taken up by LNCaP cells, while significantly fewer conjugates were taken up by the PC3 cells, consistent with our previous reports that the binding properties of A10 PSMA aptamer are maintained after conjugation to the surface of nanoparticles.[15] Because we had also shown that the intercalation of Dox within the A10 PSMA aptamer does not affect its binding properties,[17] we reasoned that the QD−Apt(Dox) conjugate would also

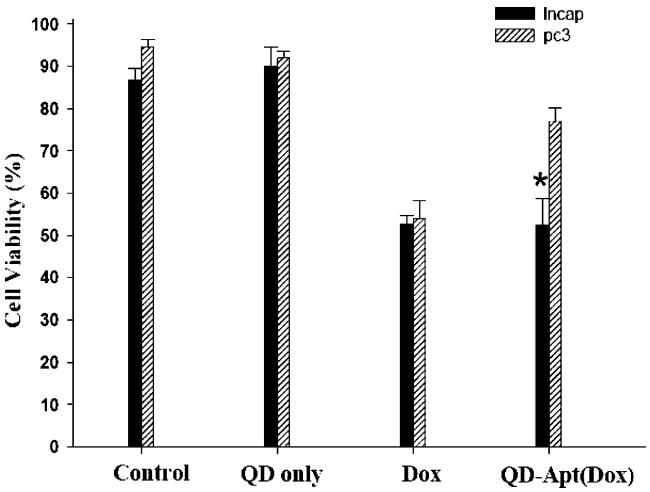

Figure 6. Growth inhibition assay (MTT). Prostate cancer cell lines, LNCaP (PSMA+) and PC3 (PSMA−), were incubated with QD alone (1.6 μM), Dox along (5 μM), or QD−Apt(Dox) conjugates (1.6 μM), for 3 h, and the cells were washed and further incubated for 24 h prior to measurement of cell viability. Asterisk indicates significant differences between LNCaP and PC3 cells, ($p < 0.005$, $n = 3$).

specifically target to LNCaP cells. Using confocal laser scanning microscopy, the fluorescence of the QD and Dox were measured after incubation of the QD−Apt(Dox) with LNCaP cells in time-course studies. LNCaP cells were incubated with 100 nM QD−Apt(Dox) for 0.5 h at 37 °C and washed twice using PBS buffer to remove free conjugates, and then cells were imaged either immediately or after 1.5 h further incubation prior to fluorescent imaging to evaluate for both the emission from Dox and QD. The data demonstrates that, with 0 h further incubation, the QD and Dox remained largely in the "OFF" state such that faint fluorescence signals from both QD and Dox were observed inside LNCaP cells (Figure 5a). This is mainly because the majority of Dox remained intercalated within the aptamer on the QD−Apt conjugate, resulting in quenching of both Dox and QD fluorescence. However, at 1.5 h of further incubation of the QD−Apt(Dox) with LNCaP cells, more Dox was released from the QD−Apt conjugates, resulting in substantial increase in the fluorescence of both QD and Dox, signifying the "ON" state of this Bi-FRET system (Figure 5b). Two possible mechanisms may induce Dox release from QD-Apt conjugates: (1) physical dissociation of Dox from the conjugates and (2) biodegradation of PSMA aptamer by lysosomal enzymes in the lysosomes. Moreover, both QD and Dox gave very sharp images of the cancer cells with low background noise, which strongly suggested that QD−aptamer(Dox) conjugate is sensitive to detect cancer cells on a single cell level in vitro.[20]

After having confirmed the feasibility of using QD−Apt-(Dox) for cancer cell imaging, we further examined the in vitro cellular cytotoxicity of the conjugate to LNCaP and PC3 cell lines respectively as compared to QD alone and Dox alone. The MTT cell proliferation assay results (Figure 6) demonstrate that, while the cytotoxicity of free Dox was equipotent against LNCaP and PC3 cells, the cytotoxicity of the QD−Apt(Dox) conjugate was significantly enhanced

against the targeted LNCaP cells as compared to the nontargeted PC3 cells (cellular viability: LNCaP 52.5 ± 1.6% versus PC3 77.2 ± 3.1%; mean ± SE, $N = 3$; probability value $p < 0.005$). Interestingly, the data showed that the cytotoxicity of QD−Apt(Dox) conjugate was nearly equipotent to that of free Dox. QD alone had no inherent cytotoxicity to LNCaP and PC3 cells (Figure 6), and we have previously reported that free PSMA aptamer has no cytotoxicity to LNCaP and PC3 cells.[17] This data suggests that the cytotoxicity of QD−Apt(Dox) results from the release of Dox molecules after endocytic uptake by LNCaP cells. Consistent with the binding specificity of QD−Apt(Dox) conjugate for PSMA expressing LNCaP cells, the observed cytotoxicity of this conjugate to PC3 cells was significantly less pronounced. The minimal cytotoxicity observed may be due to small amount of QD−Apt(Dox) conjugate by PC3 cells or alternatively by small amount of Dox that may leak into PC3 cells after being dissociated from the conjugate during incubation time (Figure 6).

In conclusion, herein we report to our knowledge the first example of a multifunctional nanoparticle that can detect cancer cells at a single cell level while intracellularly releasing a cytotoxic dose of a therapeutic agent in a reportable manner. We demonstrate the specificity and sensitivity of this cancer imaging, therapy and sensing nanoparticle conjugate system in vitro by using PCa cell lines. By functionalizing the surface of fluorescent QD with the A10 PSMA aptamer, and intercalating Dox into the double-stranded CG sequence of the A10 PSMA aptamer, we developed a targeted QD−Apt(Dox) conjugate with reversible Bi-FRET properties. The incorporation of multiple CG sequences within the stem of the aptamers may further increase the loading efficiency of Dox on these conjugates. The presence of additional Dox may enhance the self-quenching effect of QD−Apt(Dox) conjugates thereby improving their imaging sensitivity, while the higher dose of Dox may enhance the therapeutic efficacy of the conjugates. Furthermore, through the use of other disease-specific aptamers or other targeting molecules, similar multifunctional nanoparticles may potentially be developed for additional important medical applications.

Experimental Section. *Synthesis of QD-Apt Conjugate.* Carboxyl core−shell CdSe/ZnS QD (40 μL, 0.6 nM; Evitag, Dunedin, FL) was activated in the presence of 60 μL (50 mM) of 1-ethyl-3-(3-dimethylaminopropyl) carbodiimide (EDC) and 30 μL (25 mM) of *N*-hydroxysuccinimide (NHS) for 15 min under gentle stirring. The resulting *N*-hydroxysuccinimide-activated QD was covalently linked to 5′-NH2 modified A10 PSMA aptamer[12,13] (QD:Aptamer mole ratio in reaction was 1:10). The reaction was carried out under gentle mixing for 1 h, at which point ethanol amine (100 mM) was added to quench the unreacted carboxyls on the QD surface for 2 h. The final QD−Apt conjugate was washed by centrifugal spin filtration, resuspended in PBS, and then characterized using gel electrophoresis.

Fluorescence Quenching of QD−Apt(Dox) Conjugate. Purified QD−Apt conjugate (1 μM) was suspended in DNAse/RNAse free water and an increasing molar ratio of Dox was serially added (0.1, 0.3, 0.6, 1, 1.5, 2.1, 2.8, 3.5, 4.5, 5.5, 7, and 8). After each addition of Dox, the solution was mixed by vortexing for 30 min, and then the fluorescence spectrum of QD was measured by using a Shimadzu RF-PC100 spectrofluorophotometer with an excitation wavelength of 350 nm and a recorded emission range of 440−560 nm. To monitor the quenching effect of Dox intercalation on the fluorescence of Dox, a fixed concentration of Dox (10 μM) was incubated with an increasing molar ratio of purified QD−aptamer conjugate for 30 min (molar ratio of 0.02, 0.04, 0.07, 0.09, 0.12, 0.14, and 0.16), and the fluorescence spectrum of Dox was measured at excitation and emission wavelength of 480 nm and 520−640 nm, respectively.

Fluorescent Microscopy. Prostrate cancer cell lines LNCaP and PC3 cells were grown in eight-well microscope chamber slides in RPMI-1640 and Ham's F-12K medium, respectively, both supplemented with 100 units/mL of aqueous penicillin G, 100 μg/mL of streptomycin, and 10% fetal bovine serum (FBS) at concentrations to allow 70% confluence in 24 h (i.e., 40 000 cells/ cm^2). On the day of the experiments, cells were washed with prewarmed PBS buffer and incubated with prewarmed fresh media for 30 min before the addition of QD−Apt or QD−Apt(Dox) conjugates (100 nM) ($n = 4$). Cells were incubated with the conjugates for 0.5−2 h at 37 °C, washed two times with PBS (300 μL per well), fixed with 4% formaldehyde, mounted with nonfluorescent mounting medium (Vector Laboratory, Inc., Burlingame, CA), and imaged using confocal laser scanning microscopy (Carl Zeiss LSM 510, DAPI long pass filter set was used for QD imaging, and rhodamine filter set was used for Dox imaging).

MTT Cell Viability Assay. The prostate LNCaP and PC3 cell lines were grown in 96-well plates in RPMI-1640 and Ham's F-12K medium, respectively, both supplemented with 100 units/mL of aqueous penicillin G, 100 μg/mL of streptomycin, and 10% FBS at concentrations to allow 70% confluence in 24 h (i.e., 40 000 cells/cm^2). On the day of experiments, cells were washed with prewarmed PBS buffer and incubated with prewarmed fresh media for 30 min before the addition of QD−Apt(Dox) conjugate (1.6 μM), free QD (1.6 μM), or free Dox (5 μM). Cells were incubated with the conjugates for 3 h at 37 °C, washed two times with PBS (1 mL per well), and further incubated in fresh growth media for a total of 72 h. Cell viability was assessed colorimetrically with the MTT reagent (ATCC) following the standard protocol provided by the manufacturer. The absorbance was read with a microplate reader at 570 nm.

Acknowledgment. This work is supported by USA National Institute of Health grant CA119349 (R.L. and O.C.F.) and EB003647 (O.C.F.), and Korea Science and Technology Foundation grant R01-2006-000-10818-0 (S.J.).

References

(1) Michalet, X.; Pinaud, F. F.; Bentolila, L. A.; Tsay, J. M.; Doose, S.; Li, J. J.; Sundaresan, G.; Wu, A. M.; Gambhir, S. S.; Weiss, S. *Science* **2005**, *307*, 538.
(2) Medintz, I. L.; Uyeda, H. T.; Goldman, E. R.; Mattoussi, H. *Nat. Mater.* **2005**, *4*, 435.

(3) Gopalakrishnan, G.; Danelon, C.; Izewska, P.; Prummer, M.; Bolinger, P.-Y.; Geissbüler, I.; Demurtas, D.; Dubochet, J.; Vogel, H. A*ngew. Chem., Int. Ed.* **2006**, *45*, 5478.
(4) Yao, J.; Larson, D. R.; Vishwasrao, H. D.; Zipfel, W. R.; Webb, W. W. *Proc. Natl. Acad. Sci. U.S.A.* **2005**, *102*, 14284.
(5) Medintz, I. L.; Clapp, A. R.; Mattoussi, H.; Goldman, E. R.; Fisher, B.; Mauro, J. M. *Nat. Mater.* **2003**, *2*, 630.
(6) Chu, T. C.; Shieh, F.; Lavery, L. A.; Levy, M.; Richards-Kortum, R.; Korgel, B. A.; Ellington, A. D. *Biosens. Bioelectron.* **2006**, *21*, 1859.
(7) Young, S. H.; Rozengurt, E. *Am. J. Physiol. Cell Physiol.* **2006**, *290*, C728.
(8) Chen, A. A.; Derfus, A. M.; Khetani, S. R.; Bhatia, S. N. *Nucleic Acids Res.* **2005**, *33*, e190.
(9) Tan, W. B.; Jiang, S.; Zhang, Y. *Biomaterials* **2007**, *28*, 1565.
(10) Albers, A. E.; Okreglak, V. S.; Chang, C. J. *J. Am. Chem. Soc.* **2006**, *128*, 9640.
(11) Myong, S.; Rasnik, I.; Joo, C.; Lohman, T. M.; Ha, T. *Nature* **2006**, *437*, 1321.
(12) Brody, E. N.; Gold, L. *J. Biotechnol.* **2000**, *74*, 5.
(13) Fan, P.; Suri, A. K.; Fiala, R.; Live, D.; Patel, D. J. *J. Mol. Biol.* **1996**, *258*, 480.
(14) Vyawahare, S.; Eyal, S.; Mathews, K. D.; Quake, S. R. *Nano Lett.* **2004**, *4*, 1035.
(15) Farokhzad, O. C.; Jon, S.; Khademhosseini, A.; Tran, T.-N. T.; LaVan, D. A.; Langer, R. *Cancer Res.* **2004**, *64*, 7668.
(16) Lupold, S. E.; Hicke, B. J.; Lin, Y.; Coffely, D. S. *Cancer Res.* **2002**, *62*, 4029.
(17) Bagalkot, V.; Farokhzad, O. C.; Langer, R.; Jon, S. *Angew. Chem., Int. Ed.* **2006**, *45*, 8149.
(18) Valentini, L.; Nicolella, V.; Vannini, E.; Menozzi, M.; Penco, S.; Arcamone, F. *Farmaco, Ed. Sci.* **1985**, *40*, 377.
(19) Haj, H. T.; Salerno, M.; Priebe, W.; Kozlowski, H.; Garnier-Suillerot, A. *Chem. Biol. Interact.* **2003**, *145*, 349.
(20) Patil, S. D.; Rhodes, D. G; Burgess, D. J. *AAPS J.* **2005**, *7*, E61.

NL071546N